Carbohydrate Polymers 288 (2022) 119387

Contents lists available at ScienceDirect

Carbohydrate Polymers

journal homepage: www.elsevier.com/locate/carbpol

Green synthesis and chemometric characterization of hydrophobic xanthan matrices: Interactions with phenolic compounds

Max Petitjean, Nerea Lamberto, Arantza Zornoza, José Ramón Isasi *

Department of Chemistry, University of Navarra, 31080 Pamplona, Spain

ARTICLE INFO

Keywords:
Cyclodextrins
Xanthan gum
Principal component analysis
Lignin
Locust bean gum
Chitosan

ABSTRACT

Polysaccharides such as xanthan, locust bean gum or chitosan are easily crosslinked and purified using citric acid in an ecofriendly process. In order to achieve an improved sorption capability towards hydrophobic solutes, β-cyclodextrin, a cyclic oligosaccharide, and lignin, a natural aromatic polymer, are incorporated in the same process. Once crosslinked, the influence of these on the sorption capacities towards model solutes has been assessed by comparing the sorption isotherms of matrices with or without the hydrophobic modifications. The sorption capacities of these materials for different phenolic compounds have also been tested to ascertain their efficiencies as a function of their affinities to β-cyclodextrin cavities and/or their partition coefficients. In addition, these functionalized carbohydrate matrices were successfully characterized by principal component analysis, which is a useful tool to select the most appropriate polymers to interact with a specific molecule.

1. Introduction

The design of novel materials needs to become as 'green' as possible in order to prevent further pollution of the planet. The use of biomass raw materials is therefore advisable, provided that their physico-chemical properties are appropriate, because of their biodegradability.

In the last decades, the trends in environmental engineering are shifting towards the development of sustainable and eco-friendly technologies for waste water treatment. Their advantages are undoubted with respect to those aspects. Non-conventional green adsorbents include industrial by-products, agro-food wastes, natural products (such as clays, hemp, flax, and cotton), and biological materials including plants, algae, and biopolymers (Grégorio Crini et al., 2018). In particular, when compared to conventional activated carbons and synthetic ion-exchange resins, polysaccharide-based adsorbents offer advantages in cost, versatility, efficiency, selectivity, and regeneration (Oladoja et al., 2017). In addition to their uses in water treatment processes, the design of green sorbents presents other possibilities in the agro-food sector: valorization of residues and formulation of safer controlled-release agrochemicals, for instance (Campos et al., 2014).

Many natural polysaccharides, coming from bacterial, animal or vegetal origins, possess interesting characteristics as hydrogels and can be employed for sorption and/or delivery processes when used by themselves or combined through crosslinking reactions. In particular, citric acid is a sustainable triacid allowing, by means of a low energy reaction, the crosslinking of any polysaccharides by facile esterification reactions (Awadhiya et al., 2016; Bueno et al., 2013; Salihu et al., 2021).

The hydrophilic nature of polysaccharide-based adsorbents, swellable in water and allowing a fast diffusion of the target molecules, are advantageous when compared to the performance of synthetic resins and activated carbons. The addition of hydrophobic moieties to the crosslinked polysaccharide gels will provide them with the amphiphilic character required to efficiently trap non-polar pollutants. Cyclodextrin and lignin will be the hydrophobic modifiers tested and compared in this investigation.

Cyclodextrins are a family of natural cyclic oligosaccharides, mainly composed of 6, 7 or 8 glucose unit molecules (known as α-, β- and γ-cyclodextrin, respectively). Their cyclic configuration creates a hydrophobic core, allowing complexation with certain hydrophobic molecules and moieties. Their saccharide composition confers them, at the same time, a hydrophilic character and the possibility of a facile crosslinking thanks to their hydroxyl groups. Thus, it is also feasible to prepare cyclodextrin polymers in the presence of an appropriate crosslinker. Cyclodextrins can constitute the basic unimer to produce a nanosponge (Caldera et al., 2017), but also a grafted adjuvant, to create novel materials with a new functionality (Medronho et al., 2013). These products could be used in the medical sector, food technologies (Petitjean, García-Zubiri, & Isasi, 2020) or water decontamination processes

* Corresponding author.
E-mail address: jrisasi@unav.es (J.R. Isasi).

https://doi.org/10.1016/j.carbpol.2022.119387
Received 25 September 2021; Received in revised form 10 March 2022; Accepted 18 March 2022
Available online 23 March 2022

(Grégorio Crini, 2021).

Lignin is a heterogeneous aromatic biopolymer, the second most abundant in the plant kingdom. This macromolecule possesses a three-dimensional structure, average masses of about 10,000 Da, and a wide diversity of chemical groups (phenolic, hydroxyl, methoxy, …). It is mainly composed of three types of blocks: *p*-hydroxyphenyl, guaiacyl and syringyl units linked with different junctions (Xu & Ferdosian, 2017). Due to its natural origin, biodegradability and physico-chemical properties, it is used for medical applications such as wound dressing or drug delivery (Spiridon, 2020), but also for renewable energy usages (Espinoza-Acosta et al., 2018) and environmental purposes as a heavy metal sorbent (Ge & Li, 2018) or for dye removal (Domínguez-Robles et al., 2018). The Kraft process, used to separate lignin from wood using sodium sulfide in basic media, is the largest source of technical lignin (Wickham et al., 2019). Besides the modification of lignin by adding certain functionalities to its structure, other biopolymers such as starch (Shi & Li, 2016), chitosan (Crouvisier-Urion et al., 2019) and xanthan (Raschip et al., 2013) have been used as starting structures to create novel materials by mixing/crosslinking them with lignin.

In two previous works, we have prepared green sorbents using natural building blocks and solventless procedures: different hydrophilic polysaccharide matrices were functionalized with cyclodextrin to incorporate the hydrophobic cavities suitable to entrap molecules of interest (Petitjean, Aussant, et al., 2020; Petitjean & Isasi, 2021). Our first work was aimed to find the most suitable (low-cost, green and facile) conditions to prepare the matrices. In our second step, we found remarkable differences with regard to the influence of the polysaccharide matrices in the mechanisms of the interaction with certain model molecules. We selected three polysaccharides for the first part of this study: xanthan, locust bean gum, and chitosan, due to their diverse structures and properties.

Xanthan is a branched polysaccharide produced by *Xanthomonas campestris* bacteria. Its main chain is composed of D-glucose, substituted every two units with a glucuronic acid moiety between two mannoses, the last one finishing with a pyruvate function (García-Ochoa et al., 2000). Locust bean gum is also a natural branched polysaccharide, extracted from the seed of the carob fruit, and composed of a skeleton of mannose units with a galactose branch every four units. The aqueous solutions of these two polysaccharides present interesting rheological properties for food or medical purposes (Barak & Mudgil, 2014). Chitosan is a derivative from chitin, a natural polysaccharide obtained from exoskeleton of Crustacea. This linear copolymer is composed of glucosamine and *N*-acetyl-glucosamine units. Its antibacterial properties, as well as its bioactivity and biocompatibility make it usable in the biomedical field, but also in other sectors such as the textile industry and environmental chemistry (Morin-Crini et al., 2019).

As mentioned above, the efficiency and mechanisms of the sorption process were investigated by using a single model molecule. Nevertheless, the tailoring of novel green sorbents is one of their most interesting features, so their efficient performance with respect to a model sorbate is not sufficient to ascertain their potential. In addition, cyclodextrins are not the only hydrophobic green modifiers of interest. In the present investigation, we hypothesize that cyclodextrin and lignin hydrophobic functionalizations using natural building blocks by means of a solventless procedure will also produce useful sorbents to entrap phenolic compounds. The selection of this family of chemicals is due to two reasons: the interest of polyphenols as bioactive compounds is undisputed and, on the other hand, many water pollutants also belong to this group. The insights into the mechanisms of the interactions will be studied by testing the affinity of these matrices towards twenty phenolic compounds using principal component analysis and other chemometric procedures in order to relate molecular properties of the sorbates with their corresponding sorption capacities in the different carbohydrate matrices.

2. Experimental section

2.1. Materials

Kraft lignin (BioPiva 190, UPM, mol. wt. of 5000 Da), β-cyclodextrin (Wacker, humidity 12.5%), xanthan gum (Sigma Aldrich, lot SLBG3388V), locust bean gum (Sigma Aldrich, lot SLBC7065V), chitosan (deacetylation degree of 90% measured by NMR-^{1}H in D_2O with 2% HCl, Bruker Advance 400 MHz), citric acid (Panreac AppliChem) and dibasic sodium phosphate ($Na_2HPO_4 \geq 98\%$) were used as received to prepare the crosslinked resins. The characterization data of the lignin sample (Dastpak et al., 2020) and the polysaccharides used in this work can be found in the Supplementary Data section (Table S1 and Fig. S1).

Sorption analyses were performed with phenolphthalein (Merck, 99%) and 19 other aromatic compounds (see Table 1).

2.2. Methods

2.2.1. Synthesis procedure

The polysaccharide matrices were prepared by mixing the raw materials, namely, citric acid as a crosslinker (1.30 g), sodium phosphate dibasic as a catalyst (0.28 g), a selected polysaccharide (2.87 g) or a 1:1 (w/w) polysaccharide/β-cyclodextrin mixture, plus Kraft lignin (0.50 g), in a mortar (see Scheme 1 and Table S2), crushing them together to disperse them into a uniform powder and crosslink them thermally at 170 °C for 45 min (Memmert UN-30 oven). In this design, β-cyclodextrin, which is a carbohydrate (with its unique hydrophobic complexation capabilities), has been considered as a replacement of the other polysaccharides while lignin is a modifier of the crosslinked networks (i.e. a hydrophobic additive). A first washing with water (100 mL) is carried out to separate the insoluble and soluble fractions (the latter studied by size exclusion chromatography, see below). After this filtration, a second rinsing of the insoluble solid is performed using an acetone/water mixture (70/30, v/v, 100 mL) to solubilize and wash away the unreacted Kraft lignin. Finally, a third washing with water (100 mL) allows us to eliminate the last residues (including acetone from the previous step) present in the matrices. The insoluble fractions are then heated up to 102 °C during 24 h to eliminate the humidity and pulverized using a Retsch MM300 ball mill for 30 s (some micrographs are shown in the Supplementary Data section). Final yields are calculated by weighing the mass of the dried final products.

Nomenclature: the abbreviations used for the matrices produced in this work include the letters "L" and "β", to indicate **l**ignin and **β**-cyclodextrin functionalizations, respectively, followed by "c",

Table 1
Aromatic compounds used in this work, code numbers, abbreviations and sources (see other properties in the Supplementary data section, Table S1A).

Code number	Name	Abbreviation	Source, purity
1	3-Nitrophenol	3nPh	Sigma (China), 99%
2	4-Nitrophenol	4nPh	Sigma (India), 99%
3	Guaiacol	Gua	Sigma (USA)
4	4-Ethylguaiacol	4etGua	Sigma (China), 98%
5	Phenol	Ph	Panreac (Spain), 99.5%
6	4-Ethylphenol	4etPh	Sigma (China), 99%
7	1-Naphthol	1-NOH/1-N	Merck (Germany), 99%
8	Caffeine	Caff	Guinama (Spain), 99.7%
9	Caffeic acid	CaffAc	Sigma (China), 98%
10	Salicylic acid	SalAc	Panreac (Spain), 99.5%
11	*meta*-Cresol	mCr	Sigma (Germany), 99%
12	*ortho*-Cresol	oCr	Sigma (Germany), 99%
13	*para*-Cresol	pCr	Sigma (USA), 99%
14	Methylparaben	metPHB	Sigma (USA)
15	Ethylparaben	etPHB	Sigma (USA)
16	Propylparaben	prPHB	Sigma (USA)
17	Eugenol	Eug	Sigma (Germany), 99%
18	Tyrosol	Tyr	Sigma (USA), 98%
19	Vanillin	Van	Panreac (Spain), 99%

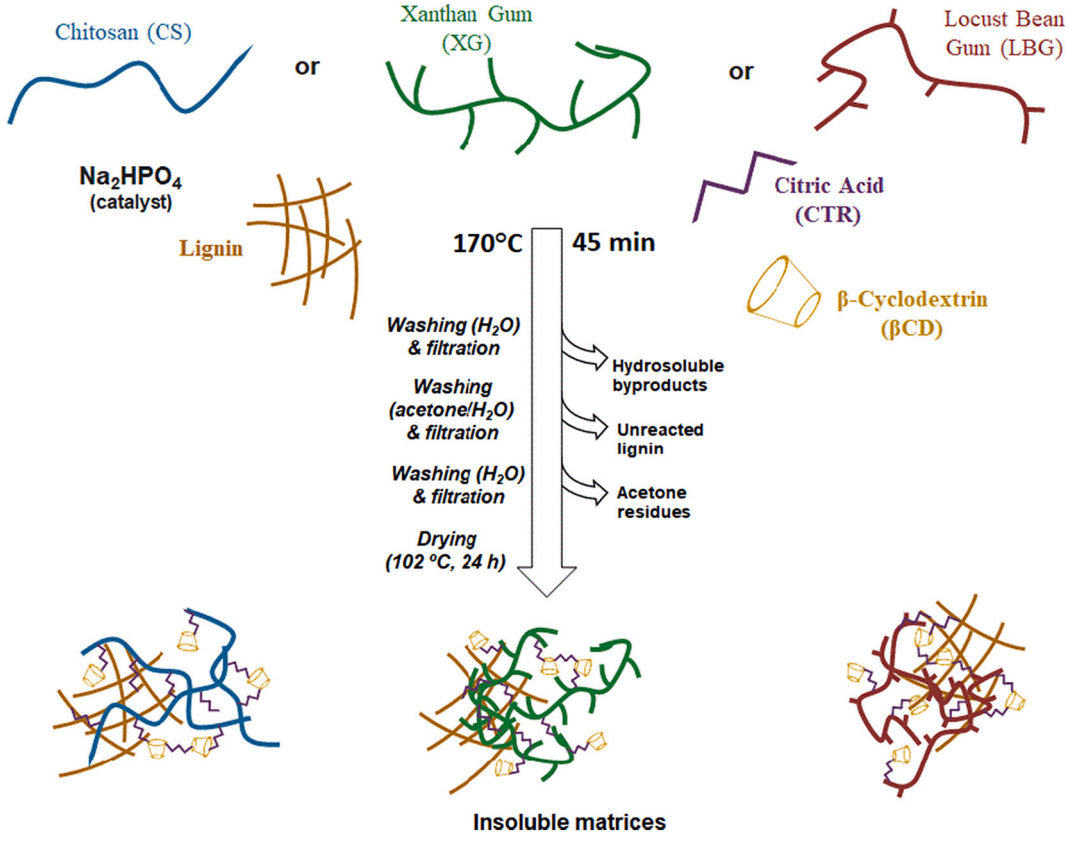

Scheme 1. Synthesis procedure of the insoluble crosslinked matrices.

symbolizing the **c**itric acid **c**rosslinker (common to all samples), plus a last uppercase letter corresponding to the polysaccharides: "X" for **x**anthan, "G" for locust bean **g**um, and "C" for **c**hitosan (see Tables 2 and S2).

2.2.2. Characterization of the matrices

Dialysis of soluble byproducts and size exclusion chromatography (SEC). The water soluble byproducts were collected and dialyzed through Spectra/Por cellulosic membranes (MWCO 6-8000, Spectrum Labs) in 1 L of distilled water during 24 h (twice). The internal and external fractions recovered are concentrated with a rotary evaporator Büchi R-200. To analyze the reaction and washing processes, a Waters 600 Controller device was employed, attached to a Waters 2414 refractive index detector and Waters 996 photodiode array detector, and an autosampler Waters 717 Plus. The column employed was a TSK-Gel Alpha 5000 (Tosoh Bioscience) calibrated with polyethylene oxide standards, and the flow rate was 1 mL/min.

Carbonyl and lignin contents by infrared spectroscopy. The insoluble crosslinked matrices were analyzed using a Shimadzu IRAffinity-1S instrument coupled with a Golden Gate™ attenuated total reflectance

Table 2
Characterization of citrate crosslinked (**c**) polysaccharide (**X**: xanthan, **G**: locust bean gum, **C**: chitosan) matrices functionalized with lignin (**L**) and β-cyclodextrin (**β**).

Matrix	CD_{eq}[a]	%lig[b]	−COOH[c]	Carbox.[d]	%CTR[e]	$q_{1\text{-}N}$ 2[f]	$q_{1\text{-}N}$ 20[f]	$q_{1\text{-}N}$ 200[f]
βc	16.5	0.0	18.7	32.6	46.2	0.26	2.60	21.13
Lβc	40.6	10.4	21.2	55.2	43.3	0.36	3.82	24.66
βcX	12.7	0.0	17.5	25.6	35.9	0.17	2.28	13.72
LβcX	33.6	8.2	20.3	44.8	35.1	0.43	3.02	19.76
cX	0.0	0.0	14.0	14.3	33.4	0.06	0.66	17.96
LcX	8.3	6.0	20.7	39.4	27.7	0.16	1.62	13.29
βcG	19.2	0.0	19.6	35.0	37.8	0.09	1.05	11.20
LβcG	30.1	9.2	18.1	29.3	36.4	0.26	2.44	17.35
cG	0.0	0.0	17.0	21.2	46.4	0.14	1.51	22.62
LcG	2.1	7.6	12.6	36.8	31.6	0.22	2.06	13.28
βcC	17.8	0.0	17.9	27.8	35.0	0.13	2.20	10.12
LβcC	30.6	11.0	9.6	28.1	37.4	0.29	2.39	15.86
cC	0.0	0.0	13.0	14.1	37.0	0.03	0.64	7.24
LcC	0.8	9.0	8.7	37.8	39.0	0.16	1.13	10.54

[a] Amount of "equivalent-available" β-cyclodextrin cavities (mg CD per g) measured using phenolphthalein (n = 3, see Table S5 for standard deviations).
[b] Amount of lignin (%) as obtained by FTIR using physical mixtures for calibration.
[c] *Contents of carboxylic acid groups (mmol per 100 g) in the matrices obtained from TBO experiments.
[d] *Carboxyl content (mmol per 100 g) after saponification measured by titration.
[e] Percent of carbonyl groups as measured by the ratio of 1710 cm^{-1}, and 1710 cm^{-1} plus 1010 cm^{-1} bands.
[f] Sorption capacity (mg/g) of 1-naphthol using 2, 20 and 200 mg/L as initial concentrations, respectively.
[*] The degree (%) of esterification (%COOR) can be calculated from **c** and **d** using Eq. (2).

(ATR) accessory device (Specac). The infrared spectra acquired were the average of 32 scans between 4000 and 600 cm^{-1} with a resolution of 4 cm^{-1}. The ratio of the intensity of the 1710 cm^{-1} band (corresponding to the citrate groups) and the sum of the intensities of that plus the one at 1010 cm^{-1} (which gives an idea of the total sugar contents) was calculated for each sample (Petitjean & Isasi, 2021). In the case of lignin, the peak located at ca. 1520 cm^{-1} was analyzed in physical mixtures of the crosslinked polysaccharides with lignin to obtain a calibration curve (see below).

Sorption analysis using liquid chromatography. For the phenolic compounds absorption studies, the high-pressure liquid chromatography (HPLC) system used was an Agilent 1100 instrument, with C18 Luna Phenomenex thermostated (40 °C) column. The flow rate was set at 1 mL/min and a gradient mode was used for the mobile phase (up to 25 min): acetonitrile from 25% to 40%, H_2O from 65% to 50%, plus methanol 10%. For the two acidic phenolic compounds, the flow rate was the same, but the mobile phase was prepared with 28% MeOH, 69% H_2O and 3% acetic acid. Four samples of each matrix (between 2 and 20 mg) were placed in 10 mL of a solution containing 20 ppm of the phenolic compounds stirred at room temperature for 5 h. Then, the solutions were filtered through 0.1 μm PVDF membranes (Durapore ®) and analyzed (see Supplementary Data for the standard deviations of these determinations).

'Available cyclodextrin' and carboxylic contents. Two colorimetric procedures were followed to obtain the amount of available cyclodextrin moieties of the matrices and to quantify the carboxylic acid contents of the samples. A 3.6×10^{-5} mol/L phenolphthalein (previously mixed with 0.4 mL of ethanol/L) solution is dissolved in a pH 10.5 buffer solution (0.1 mol/L $NaHCO_3$; 6 mol/L NaOH) (Mäkelä et al., 1987). For each polymeric matrix, samples were measured in triplicate using different weights (2, 5 and 10 mg) in 7 mL of the aforementioned solution (see also Supplementary Data section). After 24 h, the samples are centrifuged during 5 min at 10,000 rpm. Phenolphthalein absorption is measured in the supernatants using an Agilent Technologies Cary 8454 UV–Vis device, equipped with an Agilent ChemStation software.

Carboxylic acid groups. The carboxyl groups characterization was inspired by the method used by Blanchemain et al. (Blanchemain et al., 2011) but it was not possible to filtrate our powder samples to perform a desorption as suggested there. Instead, a solution of 0.2 g/L toluidine blue (TBO) was prepared in pH 10 buffer and introduced in 15 mL flasks containing 2 mg of the sample. After 24 h under mechanical agitation, the samples were centrifuged during 10 min at 4400 rpm. Supernatants were then measured at $\lambda = 634$ nm. The COOH amount in the matrix was calculated assuming the 1:1 complexation of TBO.

Carboxyl contents by titration. 50 mg of matrix were dissolved in 0.1 N NaOH (pH 12.5) during 4 h. The NaOH excess is then titrated with 0.5 N HCl in a Hach autotitrator (Titralab AT1000). The carboxyl content (mmol per 100 g) is then calculated following:

$$Carboxyl\ content\ ("titr.") = \frac{(V_b - V_a)*N}{W}*100 \quad (1)$$

where N is HCl normality (eq/L), V_a and V_b are the volumes of HCl with and without sample (mL) and W is the weight of the sample (g) (Farhat et al., 2017). Finally, the degree of esterification (%COOR) is calculated from the last two values. While TBO sorption gives us the amount of −COOH groups in the crosslinked matrix, the acid-base titration allows us to know the quantity of COOH when the matrix is dismantled. If we assume that the reticulation by citric acid modified functions is insignificant,

$$\%COOR = \frac{titr. - COOH(TBO)}{titr.}*100 \quad (2)$$

Sorption isotherms using 1-naphthol. Briefly, 10 mg of each matrix were introduced in a set of 10 mL solutions of 1-naphthol (2, 5, 10, 20, 50, 100, 150, 200, 250, 300 ppm) for 5 h. The solutions are filtered and the remaining 1-naphthol is measured by HPLC (García-Zubiri et al., 2007). The sorption model selected is Redlich-Peterson's (RP):

$$q_e = \frac{K_R C_e}{1 + a_R C_e^{\theta}} \quad (3)$$

where q_e is the amount of adsorbate in the adsorbent at equilibrium (mg/g), C_e is equilibrium concentration (mg/L), K_R (L/g) and a_R (1/mg) are the RP constants, and θ is the RP isotherm exponent.

Chemometric characterization by principal component analysis (PCA). OriginPro (2016) software was used to obtain the biplot representation (scores and loading vectors) to characterize the matrices and their interactions with the phenolic compounds. (Tables S3 and S4 include values of the loadings obtained in the corresponding analyses.)

Additional characterization data of the sorbents. Some additional characterization with regard to thermal stability, morphology and hydrophilicity of the samples can be found in the Supplementary Data section (thermogravimetric analysis, scanning electron microscopy, swelling capacities).

3. Results and discussion

3.1. Synthesis and infrared characterization of lignin functionalized polysaccharides

The first aim of the present investigation is to produce hydrophobically modified polysaccharide matrices covalently crosslinked by means of a facile and sustainable procedure. As seen in our previous studies on the solventless crosslinking of polysaccharides and β-cyclodextrin using citric acid (Petitjean, Aussant, et al., 2020; Petitjean & Isasi, 2021), the yields are lower for mixtures with lower β-cyclodextrin ratios. Citric acid reacts more efficiently with the long polysaccharide chains than with β-cyclodextrin in these solid phase reactions. Accordingly, when lignin is added to the reactive mixture, the situation becomes similar: the β-cyclodextrin/lignin crosslinking process has the lowest yield (40%); the insoluble fraction achieved for those matrices prepared with locust bean gum, chitosan or xanthan gum reach considerably higher values (up to 95% for LcX, see Fig. S2). Interestingly, for those matrices prepared with lignin, the process is even more efficient than when this ingredient is not present in the mixture, which points to a favorable crosslinking at the reaction conditions. The selection of such reaction temperature and catalyst was based on the optimization of the process in our previous work (Petitjean, Aussant, et al., 2020). It was observed that, using a reaction temperature of 170 °C, reaction times of 45 min produced the highest yields, which remained constant for longer times. As for the purification process, water is not enough to wash off all the unreacted materials and soluble byproducts because of the presence of lignin. The solubility of Kraft lignin is highest for a 70:30 acetone/water mixture (Ajao et al., 2019), so this additional step was introduced in our original facile preparation method. Size exclusion chromatographic analysis of the supernatant demonstrate the efficiency of the purification process as well as the presence of a small remaining fraction of soluble functionalized polysaccharide (see Supplementary data, Fig. S3). We can conclude that most of the original polysaccharide chains have been covalently crosslinked beyond the gel point. In addition, an appreciable fraction of unreacted β-cyclodextrin is also detected in the supernatant solution, in agreement with our previous studies (Petitjean, Aussant, et al., 2020).

The molecular structure of the synthesized crosslinked networks is obviously complex but the main chemical groups suitable for the establishment of specific interactions with phenolic solutes can be 'easily' characterized. Besides the ratio of lignin that has been successfully incorporated into the matrices, the other distinctive groups include the citrate carbonyls plus some free unreacted carboxylic acid groups, and the β-cyclodextrin cavities available for complexation. In addition, chitosan possesses its characteristic amine groups, and xanthan gum

includes some pyruvic and acetic acidic groups (Petitjean & Isasi, 2021). All these interaction sites appear immersed within a grid made of saccharides, rich in hydroxyl groups.

As shown in the case of similarly crosslinked matrices (Petitjean & Isasi, 2021), infrared spectroscopy is a reliable tool to study the chemical composition of these materials. Firstly, for the crosslinked matrices, a band at 1730 cm^{-1} shows the presence of **CO**OH/**CO**OR chemical groups. The citrate links create the 'infinite' network structure that makes the resins insoluble. For the three original polysaccharides studied in this work, only xanthan gum shows a band at 1720 cm^{-1}, which corresponds to its **CO**OH groups. For the two other carbohydrate polymers, chitosan and locust bean gum, this band is not present. In addition, the crosslinked matrices show an increase of intensity in the 1150–1250 cm^{-1} region (Fig. S4), correlated to the stretching of carbonyl bonds in COOH/COOR groups, which is not present in the original polymer chains. For each spectrum, the band located at 1010 cm^{-1} corresponds to C—O deformations. This mode is present in all the 'sugar' structures (cyclodextrins and polysaccharides) so it can serve as a reference for quantitative purposes. Finally, in the case of the chitosan spectra, the region between 1650 cm^{-1}-1550 cm^{-1} corresponds to amine and/or amide groups including the characteristic bonds originated by the Maillard reaction, an additional mechanism for the crosslinking in these polysaccharides (Petitjean & Isasi, 2021). Fig. 1 shows the curve fitting results in the 1800–1500 cm^{-1} region including all those contributions. Additionally, the spectra in the fingerprint region of the parent polysaccharides, β-cyclodextrin, citric acid and lignin, and the crosslinked resins can be found in Fig. S4 (Supplementary data section), to confirm the establishment of new covalent bonding.

The amount of lignin incorporated into the crosslinked matrices, a crucial parameter to investigate these new materials, can be easily deduced from the infrared spectra. A low intensity characteristic peak located at ca. 1510 cm^{-1}, corresponding to its aromatic C—C stretching bonds, appears partially overlapping other bands found in this region. To illustrate the procedure followed to analyze the lignin contents of the crosslinked functionalized resins, Fig. 1 shows the spectra of physical mixtures of β-cyclodextrin and lignin prepared using different ratios. By means of a calibration curve obtained from those, the amount of lignin in a given crosslinked polysaccharide can be easily interpolated, and the results are shown in Table 2.

The thermogravimetric analysis of the matrices (see Supplementary Data section) confirms the presence of lignin by an increase in the temperature of degradation for the 250–400 °C step. The degradation patterns of β-cyclodextrin and the polysaccharide (xanthan) component of the matrices are also evidently separated in the differential thermogravimetric curves.

3.2. Chemometric characterization of the matrices using principal component analysis

Aside from the fact that the cyclodextrin units do not show any characteristic chemical groups identifiable by infrared spectroscopy because they are made of glucose units, the presence of their relatively hydrophobic cavities 'makes them special'. Thanks to the specific sorption of phenolphthalein into the β-cyclodextrin cavities (Mohamed et al., 2010), it was proposed to correlate this interaction with the amount of available sites in a given matrix. Fig. 2 shows the results of such analysis for the matrices prepared in this work. As expected, for the seven lignin functionalized matrices, phenolphthalein is more efficiently absorbed in those prepared with cyclodextrin. Similar intermediate values are found for the three cyclodextrin/polysaccharide matrices. Although the literature cited above shows that this is a reliable method to analyze the cyclodextrin contents of copolymer materials, it is observed here that matrices with no β-cyclodextrin also absorb some phenolphthalein. This fact is attributed to the contribution of the lignin groups attached to the networks, so the amount of available cyclodextrin cavities would be overestimated when lignin is present. Moreover, a remarkable difference in the phenolphthalein sorption exists between matrices with or without lignin. For each polysaccharide, matrices prepared in this work without lignin present lower phenolphthalein sorptions. When phenolphthalein is used to check the availability of β-cyclodextrin cavities, lignin possesses its own sorption power. Therefore, a higher result for lignin matrices is observed, as pointed out above. These results indicate that lignin can also be used as a "molecular magnet" for phenolic molecules due to its own structure made of this same type of subunits. For this reason, we have labeled that quality in Fig. 2 as "equivalent available" β-cyclodextrin sites.

In addition to the characteristics studied so far, namely, infrared analysis of both lignin and citrate groups and the absorption of phenolphthalein, three additional analyses have been carried out to ascertain the main differences of our matrices. The carboxyl contents have been measured by chemical titration after saponification of the samples. Those values were subsequently used to obtain the degrees of esterification using the carboxylic acid data from TBO analyses (see experimental section and Table 2). Finally, 1-naphthol was employed as an alternative probe to examine the sorption behavior of the matrices, as proposed in previous works (Petitjean & Isasi, 2021). In this case, three different levels of 1-naphthol concentrations were tested, namely 2, 20 and 200 ppm (see Table 2).

Principal component analysis (PCA) is one of the most commonly used chemometric techniques. This unsupervised pattern recognition method has also been recently used to characterize sorbents (Frescura et al., 2020; Smolínski & Howaniec, 2017; Sörengård et al., 2020). In

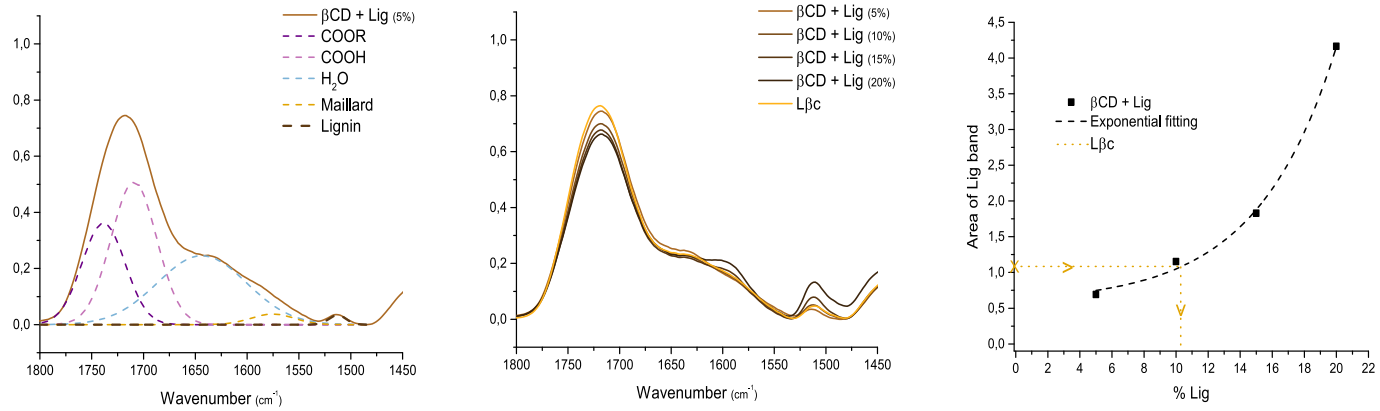

Fig. 1. Infrared spectra in the 1800–1450 cm^{-1} region of the crosslinked sample **LβcC** showing the contributions in this region, including the well resolved lignin band at 1510 cm^{-1} (left); physical mixtures of lignin and β-cyclodextrin (βCD) in different mass percent ratios including a chemically crosslinked sample **Lβc** (center); calibration curve of lignin contents using the areas of the 1510 cm^{-1} peak.

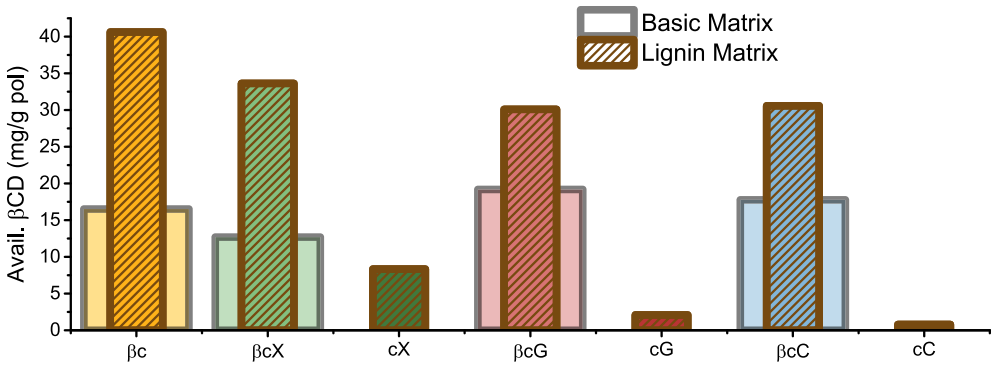

Fig. 2. "Equivalent available" β-cyclodextrin (mg/g) on lignin matrices calculated using the phenolphthalein sorption method.

this case, we are first interested in identifying the relationships between the properties analyzed so far for these crosslinked sorbents. The PCA model was prepared for the standardized matrix with all the data presented in Table 2 and Fig. S2 (i.e. 14 × 10 values, if we also include % COOR results). The data compression was effective and three principal components described 85.25% of the total data variance. The score and loading biplot is presented in Fig. 3 for the first two principal components (51.5% and 26.3% of the total variance, respectively). In this type of diagram, the eigenvectors (blue lines coming from the origin) show the correlations between every pair of characteristic properties thanks to the angle formed by the two vectors. Thus, a 90° angle implies no-connection between the parameters, while an acute angle shows a synergy or correlation, and obtuse angles imply anti-synergies (negative correlations). Assuming that, the "yield" parameter is practically forming a right angle with the percentage of lignin (i.e. no correlation) and also with the amount of ester bridges ("%COOR"), which shows that a high esterification number does not necessarily determine a high yield. On the other hand, "yield" forms close to a 180° angle with "CTR" (citrate as determined by infrared analysis). This means that a high amount of citric acid in the matrix is correlated to a low yield for that particular sample. The amount of free carboxyl groups in the matrix shows a vector close to "CTR" because both quantities are closely related, although this is not the case with "%COOR". The percentage of crosslinked bridges does not seem to depend on the total contents of citric acid. As a matter of fact, other types of crosslinking are feasible in these reaction conditions. In addition, the 'available cyclodextrin' vector is forming a low angle with 1-naphthol sorbed at the two low concentrations, "q2" and "q20" vectors, indicating that these sorptions are mainly attributable to those hydrophobic moieties. Also, the lignin vector shows a higher angle when the concentration of 1-naphthol is high ("q200"), meaning that lignin plays a more important role when there is a low concentration of this sorbate.

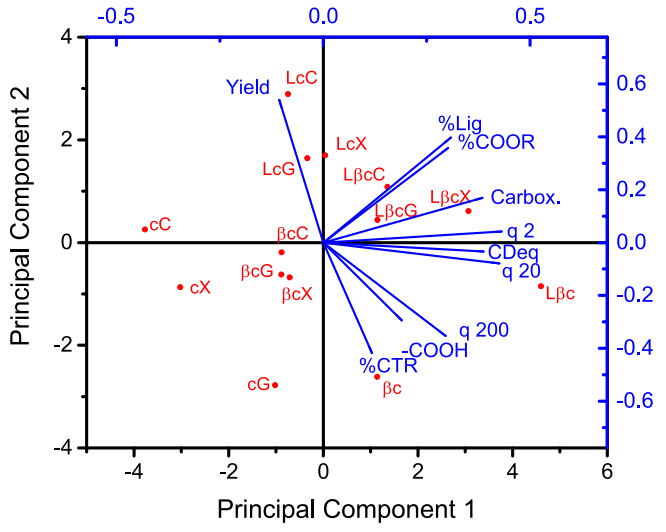

Fig. 3. Score (red) and loading (blue) biplot of the 14 matrices studied in this work using the 10 properties collected in Table 2 and Fig. S2. (For interpretation of the references to color in this figure legend, the reader is referred to the web version of this article.)

Thus, if we look closer at the scores obtained for the analyzed elements, several families are formed. First, the three lignin matrices with no cyclodextrin (LcC, LcG and LcX) appear close to the "yield" vector, meaning that these matrices have been obtained with a good yield, but they display poorer values for the other parameters. Secondly, the three lignin + cyclodextrin crosslinked polysaccharides (LβcC, LβcG and LβcX) are also close to each other, denoting that they present similar properties. In addition, Lβc (lignin plus cyclodextrin crosslinked in the absence of polysaccharides) is located on the same imaginary section beyond those two groups of samples, which indicates a close connection to them, most probably due to their lignin composition. This latter Lβc score is close to the sorption capacities q2 and q20 loading region, meaning that this is the matrix with the best sorption performance at moderate 1-naphthol concentrations, as deduced from the location of these eigenvectors. Non-lignin materials scores are on the other side of the graph, forming almost two imaginary lines parallel to the first sector described above. The family of unmodified crosslinked polysaccharides (cC, cG, cX) is forming a line, with cC closer to the yield vector and cG closer to the sorption of 1-naphthol at high concentrations (in agreement with its best sorption capacity also shown in a previous work (Petitjean & Isasi, 2021)). On the other hand, the three cyclodextrin/polysaccharide scores (βcC, βcG, βcX) are close to each other, next to the diagram center, and form another imaginary line with "βc" (crosslinked β-cyclodextrin). The first three show 'intermediate' or average properties while the latter score points to the region of the eigenvectors for highest citrate and free carboxyl contents, as expected.

3.3. Sorption isotherms using 1-naphthol as a probe

In addition to phenolphthalein, 1-naphthol has been used as a model molecule to characterize cyclodextrin networks by analyzing the corresponding sorption isotherms (García-Zubiri et al., 2007; Petitjean & Isasi, 2021). The principal component analysis presented above indicates that the choice was indeed appropriate. The eigenvectors corresponding to the sorption capacities of 1-naphthol ("q2" and "q20" in Fig. 3) are closely correlated with that of phenolphthalein sorption (labeled as 'CDeq' in Table 2 and Fig. 3). Nevertheless, when an extremely high amount of 1-naphthol is present in the solution ("q200"), the situation changes (and the eigenvector moves away). Thus, a more complex behavior is expected and the analysis of the complete sorption isotherms is mandatory. Fig. 4 shows such isotherms for the matrices prepared in this investigation. For each individual plot corresponding to

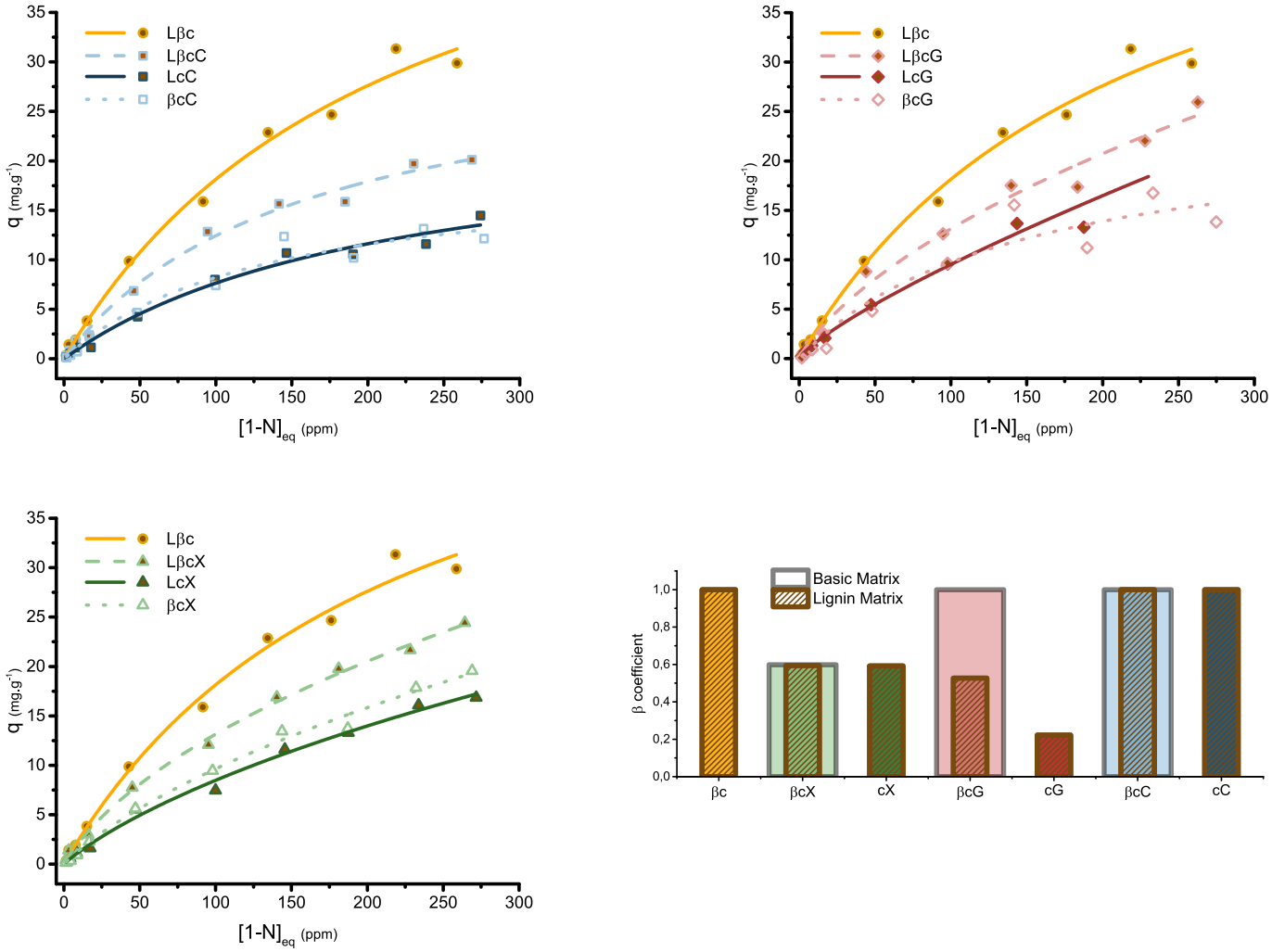

Fig. 4. 1-Naphthol isotherms fitted with Redlich-Peterson model for the three polysaccharides. Yellow dot lines: Lβc; colored dash lines: Lβc'PS'; colored dot lines: Lc'PS'; colored solid lines: βc'PS'. In blue: chitosan matrices (C), in red: locust bean gum (G), in green: xanthan matrices (X). Bottom right: RP coefficients for matrices crosslinked with (brown outline) or without (grey) lignin. (For interpretation of the references to color in this figure legend, the reader is referred to the web version of this article.)

a given polysaccharide ('PS'), if the lignin matrices are compared, Lβc possess a higher sorption capacity than the other ones, followed by Lβc'PS' and finally Lc'PS'. This agrees with the fact of a preferential sorption of this model molecule within the β-cyclodextrin cavities. Nevertheless, the isotherms corresponding to the βc'PS' samples, i.e. the lignin-free cyclodextrin/polysaccharide matrices, are very similar to those of the cyclodextrin-free lignin/polysaccharide matrices (Lc'PS'). Once again, lignin possesses its own sorption potential for this model solute as well.

The characteristics of the sorbents can be analyzed with the help of several sorption models. In particular, the Redlich-Peterson (RP) model is intermediate between the Freundlich and Langmuir isotherms. A coefficient θ in the Redlich-Peterson isotherm (see Eq. (3)) allows us to understand the relative importance of these two models in each case. Thus, when θ equals zero, the RP isotherm is similar to the Freundlich isotherm, and for values close to unity, RP corresponds to the Langmuir model. For the lignin matrices (see Fig. 4), Lβc presents a θ coefficient equal to 1, as occurs for both lignin/chitosan matrices. These sorbents behave as Langmuir-like, i.e. they are quite homogeneous with regard to the 1-naphthol sorption. On the other hand, xanthan and locust bean gum lignin matrices possess θ coefficients lower than 1. Interestingly, the θ coefficient for the xanthan matrices is the same in the three cases, even for that without lignin. For the LBG matrices, the network without lignin corresponds to a homogeneous sorbent, while that θ coefficient decrease for the other two samples.

3.4. *Interactions of the xanthan crosslinked networks with phenolic compounds*

For this last part of our investigation, we have selected the xanthan crosslinked matrices with or without lignin and cyclodextrin, which will be compared with the lignin and cyclodextrin samples crosslinked in the absence of polysaccharides. Several reasons justify this choice. First, xanthan can be produced in a controlled microbial biotechnology process to yield more uniform products, while locust bean gum production involves a somewhat problematic purification process, and chitosan may present different characteristics depending on its source and deacetylation degree. Secondly, xanthan solutions and gels generally present better properties than those of chitosan or locust bean gum. The swelling behavior of these sorbents shows a remarkable hydrophilicity of the 'pure' crosslinked xanthan (well above that of β-cyclodextrin), somewhat diminished, as expected, when the hydrophobic lignin modifications are added to the carbohydrate matrices (see Supplementary data, Fig. S7). Finally, and most importantly in this investigation, Fig. 3 shows that the LβcX score is the closest to the first principal component, which is related to the affinity to the two selected solutes, 1-naphthol and

phenolphthalein.

In addition to those two model molecules, different phenolic compounds were chosen and arranged as a function of their inclusion constants with β-cyclodextrin (*K*) and of their hydrophobicity (using the 1-octanol/water partition coefficients, *logP*) (see Fig. 5a and Table S1). The interest of phenolic compounds to test the sorption capabilities of these materials is twofold. Besides their great potential as antioxidants, we have to bear in mind their resemblance to the lignin structure. In fact, lignins are synthesized by the crosslinking of phenolic precursors, and both aromatic and hydroxyl groups are preserved in its structure (Xu & Ferdosian, 2017). Fig. 5 shows that a clear tendency can be seen for all matrices, with the highest sorption capacities found especially for large *logK* and *logP* values and decreasing fast with both characteristics. It is evident that lignin favors sorption in most cases and so does the cyclodextrin moiety. Nevertheless, specific interactions with the matrices and, possibly, steric compatibility must also play a role since some complex behavior is observed. Some values seem to be abnormally higher than others.

With the aim of ascertaining some possible hidden ordered behavior, a PCA study was also performed in this case. The loading eigenvectors (blue lines) of the PC1-PC2 graph in Fig. 6 show that all the compounds are packed, and only caffeine (labeled as '8') is excluded. Indeed, this is the only non-phenolic molecule analyzed and serves as a counterexample outlier. Thus, the first principal component (which explains 73.9% of the variance) refers to the phenolic molecule family. We can see also that some similar molecules, such as the three cresols, are not close to each other in the diagram, while others, such as the parabens, appear in similar locations. Thus, the type of phenol is more important in this classification than the hydrophobicity and the affinity with cyclodextrin.

Finally, the red dots in the biplot of Fig. 6 correspond to the six matrices studied in this case. Interestingly, those six scores occupy similar spots to those found in Fig. 3. Both classifications, obtained using different properties, produce a comparable arrangement of the crosslinked resins. As mentioned above (see Fig. 5), the lignin matrices present higher sorptions than those of the non-lignin matrices. Considering the first three principal components, Lβc sample is the closest to the group of the phenol vectors, showing that this material presents a high affinity for the phenolic compounds (those, in fact, were phenolphthalein and 1-naphthol in Fig. 3). As all the loading vectors (except "8")

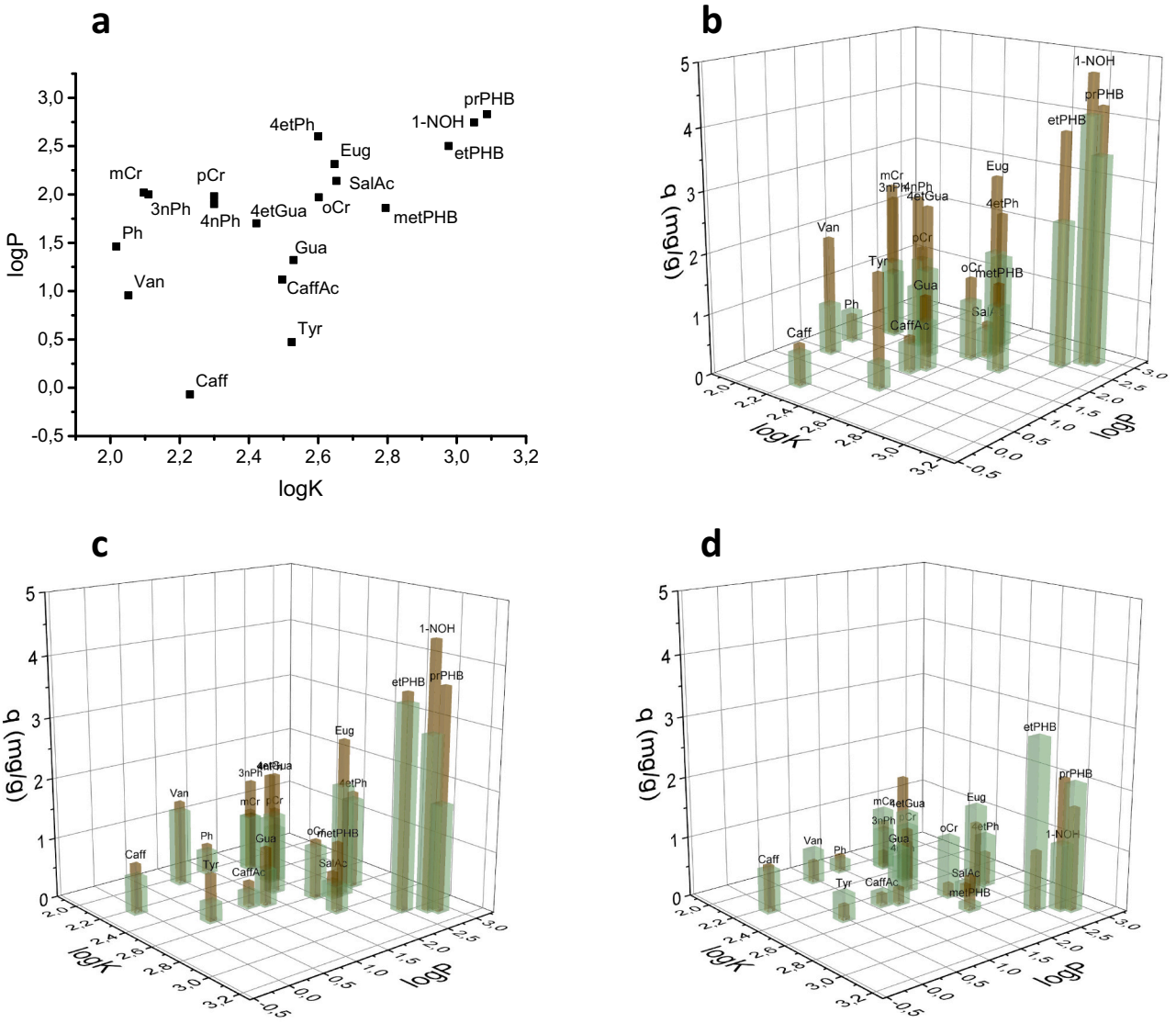

Fig. 5. Sorption capacities of phenolic compounds (in mg/g), whose *logK* and *logP* values are shown in (a) (abbreviations in Table 1), by resins βc (b), βcX (c) and cX (d) with lignin (brown columns) or without it (green). (Phenols abbreviations in Table 1; constants in Supplementary data, Table S1; n = 4, std. deviations in Table S6). (For interpretation of the references to color in this figure legend, the reader is referred to the web version of this article.)

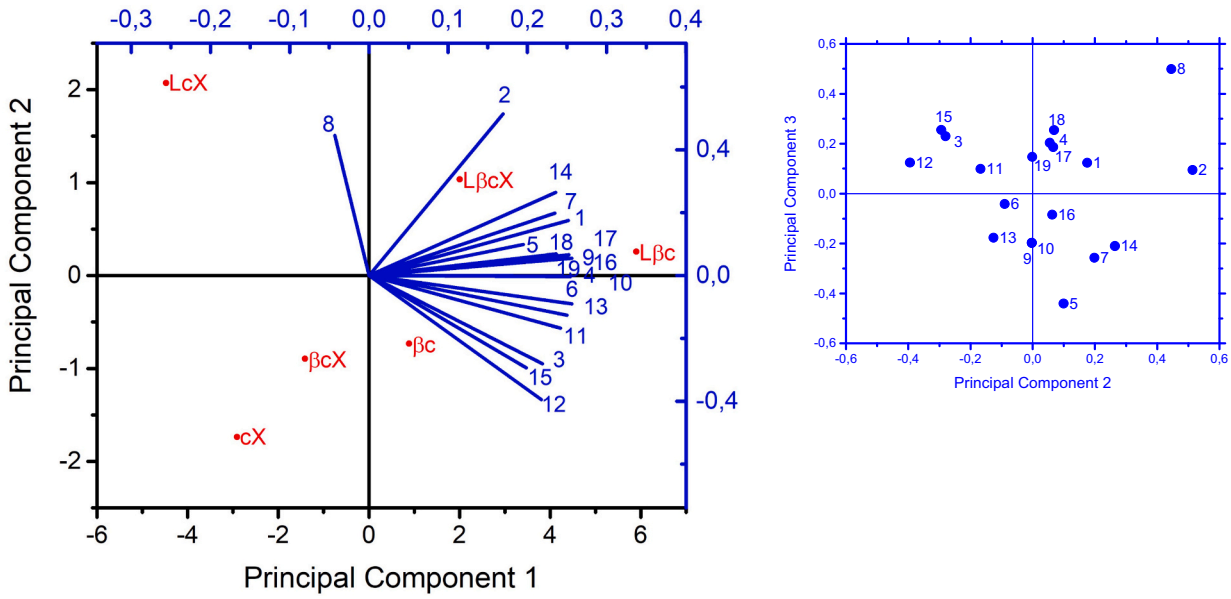

Fig. 6. Principal component analysis of the six matrices studied using the 19 aromatic compounds (see Table 1). Main diagram: PC1 vs. PC2 biplot with eigenvectors (blue) and scores (red); inset: loading plot PC2 vs. PC3. (Variances explained are 73.9% for PC1, 10.3% for PC2, 9.0% for PC3.) (For interpretation of the references to color in this figure legend, the reader is referred to the web version of this article.)

appear on the right side on the graph, the polymers on the left side correspond to those with lower sorption capacities for such molecules. Thus, this kind of biplot diagrams could be useful to select the most appropriate polymers to absorb a given molecule of interest.

4. Conclusions

This investigation has presented a facile and 'green' preparation method to produce hydrophobically modified crosslinked polysaccharide gels suitable to entrap phenolic compounds. Although xanthan matrices exhibit the best performance compared to the other two carbohydrate polymers tested, the choice will obviously depend on the particular application. These functionalized matrices preferably sorb those molecules with a high affinity towards β-cyclodextrin cavities and/or large values of the octanol-water partition coefficient, with a synergistic effect when both hydrophobic modifications are present. The use of a hydrophilic polysaccharide matrix (xanthan in particular) as a scaffold for cyclodextrin and lignin hydrophobic moieties can be useful to prepare hydrogels that would allow a fast diffusion of solutes of interest. It has been shown that the characterization of such materials using principal component analysis is an advisable statistical method that provides some valuable information both to analyze the correlation of their properties and to study their suitability for the sorption of different compounds.

CRediT authorship contribution statement

Max Petitjean: Conceptualization, Methodology, Investigation, Data curation, Formal analysis, Writing – original draft, Visualization. **Nerea Lamberto:** Methodology, Investigation. **Arantza Zornoza:** Conceptualization, Investigation, Writing – review & editing. **José Ramón Isasi:** Conceptualization, Supervision, Writing – review & editing, Project administration, Funding acquisition.

Declaration of competing interest

The authors declare that they have no known competing financial interests or personal relationships that could have appeared to influence the work reported in this paper.

Acknowledgements

The authors wish to thank Universidad de Navarra, PIUNA 2018-15 (Spain) for the financial support, to M. Domeño for his help with UV–vis and HPLC measurements and to J.I. Álvarez-Galindo for thermal analyses. M.P. thanks Asociación de Amigos (Universidad de Navarra) for his doctoral grant.

Appendix A. Supplementary data

Supplementary data to this article can be found online at https://doi.org/10.1016/j.carbpol.2022.119387.

References

Ajao, O., Jeaidi, J., Benali, M., Abdelaziz, O. Y., & Hulteberg, C. P. (2019). Green solvents-based fractionation process for kraft lignin with controlled dispersity and molecular weight. *Bioresource Technology, 291*, Article 121799. https://doi.org/10.1016/j.biortech.2019.121799

Awadhiya, A., Kumar, D., & Verma, V. (2016). Crosslinking of agarose bioplastic using citric acid. *Carbohydrate Polymers, 151*, 60–67. https://doi.org/10.1016/j.carbpol.2016.05.040

Barak, S., & Mudgil, D. (2014). Locust bean gum: Processing, properties and food applications-A review. *International Journal of Biological Macromolecules, 66*, 74–80. https://doi.org/10.1016/j.ijbiomac.2014.02.017

Blanchemain, N., Aguilar, M. R., Chai, F., Jimenez, M., Jean-Baptiste, E., El-Achari, A., Martel, B., Hildebrand, H. F., & San Roman, J. (2011). Selective biological response of human pulmonary microvascular endothelial cells and human pulmonary artery smooth muscle cells on cold-plasma-modified polyester vascular prostheses. *Biomedical Materials, 6*(6). https://doi.org/10.1088/1748-6041/6/6/065003

Bueno, V. B., Bentini, R., Catalani, L. H., & Petri, D. F. S. (2013). Synthesis and swelling behavior of xanthan-based hydrogels. *Carbohydrate Polymers, 92*(2), 1091–1099. https://doi.org/10.1016/j.carbpol.2012.10.062

Caldera, F., Tannous, M., Cavalli, R., Zanetti, M., & Trotta, F. (2017). Evolution of cyclodextrin nanosponges. *International Journal of Pharmaceutics, 531*(2), 470–479. https://doi.org/10.1016/j.ijpharm.2017.06.072

Campos, E. V. R., de Oliveira, J. L., Fraceto, L. F., & Singh, B. (2014). Polysaccharides as safer release systems for agrochemicals. *Agronomy for Sustainable Development, 35*(1), 47–66. https://doi.org/10.1007/s13593-014-0263-0

Crini, G. (2021). Cyclodextrin–epichlorohydrin polymers synthesis, characterization and applications to wastewater treatment: A review. *Environmental Chemistry Letters*. https://doi.org/10.1007/s10311-021-01204-z, 0123456789.

Crini, G., Lichtfouse, E., Wilson, L. D., & Morin-Crini, N. (2018). Adsorption-oriented processes using conventional and non-conventional adsorbents for wastewater treatment. In G. Crini, & E. Lichthouse (Eds.), *Green adsorbents for pollutant removal : Fundamentals and design* (pp. 23–72). Springer Nature Switzerland AG. https://books

.google.pt/books?id=BVhiDwAAQBAJ&dq=model+Spahn+%26+Schlunder+sorption&hl=pt-PT&source=gbs_navlinks_s.
Crouvisier-Urion, K., Da Silva, R., Farias, F., Arunatat, S., Griffin, D., Gerometta, M., Rocca-Smith, J. R., Weber, G., Sok, N., & Karbowiak, T. (2019). Functionalization of chitosan with lignin to produce active materials by waste valorization. *Green Chemistry, 21*(17), 4633–4641. https://doi.org/10.1039/c9gc01372e
Dastpak, A., Lourençon, T. V., Balakshin, M., Farhan Hashmi, S., Lundström, M., & Wilson, B. P. (2020). Solubility study of lignin in industrial organic solvents and investigation of electrochemical properties of spray-coated solutions. *Industrial Crops and Products, 148*, Article 112310. https://doi.org/10.1016/j.indcrop.2020.112310
Domínguez-Robles, J., Peresin, M. S., Tamminen, T., Rodríguez, A., Larrañeta, E., & Jääskeläinen, A. S. (2018). Lignin-based hydrogels with "super-swelling" capacities for dye removal. *International Journal of Biological Macromolecules, 115*, 1249–1259. https://doi.org/10.1016/j.ijbiomac.2018.04.044
Espinoza-Acosta, J. L., Torres-Chávez, P. I., Olmedo-Martínez, J. L., Vega-Rios, A., Flores-Gallardo, S., & Zaragoza-Contreras, E. A. (2018). Lignin in storage and renewable energy applications: A review. *Journal of Energy Chemistry, 27*(5), 1422–1438. https://doi.org/10.1016/j.jechem.2018.02.015
Farhat, W., Venditti, R., Mignard, N., Taha, M., Becquart, F., & Ayoub, A. (2017). Polysaccharides and lignin based hydrogels with potential pharmaceutical use as a drug delivery system produced by a reactive extrusion process. *International Journal of Biological Macromolecules, 104*, 564–575. https://doi.org/10.1016/j.ijbiomac.2017.06.037
Frescura, L. M., de Menezes, B. B., Duarte, R., & da Rosa, M. B. (2020). Application of multivariate analysis on naphthalene adsorption in aqueous solutions. *Environmental Science and Pollution Research, 27*(3), 3329–3337. https://doi.org/10.1007/s11356-019-07278-1
García-Ochoa, F., Santos, V. E., Casas, J. A., & Gomez, E. (2000). Xanthan gum: Production, recovery, and properties. *Biotechnology Advances, 18*, 549–579. https://doi.org/10.1016/S0734-9750(00)00050-1
García-Zubiri, Í. X., González-Gaitano, G., & Isasi, J. R. (2007). Isosteric heats of sorption of 1-naphthol and phenol from aqueous solutions by β-cyclodextrin polymers. *Journal of Colloid and Interface Science, 307*(1), 64–70. https://doi.org/10.1016/j.jcis.2006.10.076
Ge, Y., & Li, Z. (2018). Application of lignin and its derivatives in adsorption of heavy metal ions in water: A review. *ACS Sustainable Chemistry and Engineering, 6*(5), 7181–7192. https://doi.org/10.1021/acssuschemeng.8b01345
Mäkelä, M., Korpela, T., & Laakso, S. (1987). Colorimetric determination of β-cyclodextrin: Two assay modifications based on molecular complexation of phenolphtalein. *Journal of Biochemical and Biophysical Methods, 14*(2), 85–92. https://doi.org/10.1016/0165-022X(87)90043-1
Medronho, B., Andrade, R., Vivod, V., Ostlund, A., Miguel, M. G., Lindman, B., Voncina, B., & Valente, A. J. M. (2013). Cyclodextrin-grafted cellulose: Physico-chemical characterization. *Carbohydrate Polymers, 93*(1), 324–330. https://doi.org/10.1016/j.carbpol.2012.08.109
Mohamed, M. H., Wilson, L. D., & Headley, J. V. (2010). Estimation of the surface accessible inclusion sites of β-cyclodextrin based copolymer materials. *Carbohydrate Polymers, 80*(1), 186–196. https://doi.org/10.1016/j.carbpol.2009.11.014
Morin-Crini, N., Lichtfouse, E., Torri, G., & Crini, G. (2019). Applications of chitosan in food, pharmaceuticals, medicine, cosmetics, agriculture, textiles, pulp and paper, biotechnology, and environmental chemistry. *Environmental Chemistry Letters, 17*(4), 1667–1692. https://doi.org/10.1007/s10311-019-00904-x
Oladoja, N. A., Unuabonah, E. I., Amuda, O. S., & Kolawole, O. M. (2017). Polysaccharides as a green and sustainable resources for water and wastewater treatment. In *Biobased Polymers*. Springer Nature. http://link.springer.com/10.1007/978-3-319-56599-6.
Petitjean, M., Aussant, F., Vergara, A., & Isasi, J. R. (2020). Solventless crosslinking of chitosan, xanthan, and locust bean gum networks functionalized with β-cyclodextrin. *Gels, 6*(4), 1–13. https://doi.org/10.3390/gels6040051
Petitjean, M., García-Zubiri, I. X., & Isasi, J. R. (2020). In *Cyclodextrin-based polymers for food and pharmaceutical applications: A historical review* (pp. 281–304). https://doi.org/10.1007/978-3-030-49308-0_6
Petitjean, M., & Isasi, J. R. (2021). Chitosan, xanthan and locust bean gum matrices crosslinked with β-cyclodextrin as green sorbents of aromatic compounds. *International Journal of Biological Macromolecules, 180*, 570–577. https://doi.org/10.1016/j.ijbiomac.2021.03.098
Raschip, I. E., Hitruc, G. E., Vasile, C., & Popescu, M. C. (2013). Effect of the lignin type on the morphology and thermal properties of the xanthan/lignin hydrogels. *International Journal of Biological Macromolecules, 54*(1), 230–237. https://doi.org/10.1016/j.ijbiomac.2012.12.036
Salihu, R., Abd Razak, S. I., Ahmad Zawawi, N., Rafiq Abdul Kadir, M., Izzah Ismail, N., Jusoh, N., Riduan Mohamad, M., & Hasraf Mat Nayan, N. (2021). Citric acid: A green cross-linker of biomaterials for biomedical applications. *European Polymer Journal, 146*, Article 110271. https://doi.org/10.1016/j.eurpolymj.2021.110271
Shi, R., & Li, B. (2016). Synthesis and characterization of cross-linked starch/lignin film. *Starch/Staerke, 68*(11–12), 1224–1232. https://doi.org/10.1002/star.201500331
Smolínski, A., & Howaniec, N. (2017). Analysis of porous structure parameters of biomass chars versus bituminous coal and lignite carbonized at high pressure and temperature-a chemometric study. *Energies, 10*(10), 28–30. https://doi.org/10.3390/en10101457
Sörengård, M., Östblom, E., Köhler, S., & Ahrens, L. (2020). Adsorption behavior of per- and polyfluoralkyl substances (PFASs) to 44 inorganic and organic sorbents and use of dyes as proxies for PFAS sorption. *Journal of Environmental Chemical Engineering, 8*(3), Article 103744. https://doi.org/10.1016/j.jece.2020.103744
Spiridon, I. (2020). Extraction of lignin and therapeutic applications of lignin-derived compounds.A review. *Environmental Chemistry Letters, 18*(3), 771–785. https://doi.org/10.1007/s10311-020-00981-3
Wickham, J., Stehman, S., Gass, L., Dewitz, J., Sorenson, D., Granneman, B., Ross, R., & Baer, L. (2019). EPA public access. *Advances in Ecological Research, 60*, 1–24. https://doi.org/10.1002/bbb.1913.Submit
Xu, C., & Ferdosian, F. (2017). Structure and properties of lignin. In *Conversion of lignin into bio-based chemicals and materials, green chemistry and sustainable technology* (pp. 1–12). Springer-Verlag GmbH. https://doi.org/10.1007/978-3-662-54959-9_1.